Building the 3-D integral DMO operator in the slant-stack domain

Yalei Sun and Tariq Alkhalifah, Stanford University*

SUMMARY

We propose a 3-D integral dip-moveout (DMO) approach based on constructing the DMO operator in the slant-stack domain. The kinematics of the operator is first computed in the ray parameter domain and described as three parametric functions for the zero-offset trace location x_0-, y_0-, and zero-offset traveltime t_0. 3-D slant-stack transform is used to merge the three functions into one that defines the same operator in the slant-stack domain. Each input sample is smeared as a sinc function onto the output panel in the slant-stack domain, along the DMO operator trajectory. Then, an accurate and efficient inverse 3-D slant-stack transform reconstructs the data in the conventional time-space domain. Two significant advantages arise from this implementation. First, it can kinematically and dynamically handle triplications associated with $v(z)$ media; second, this integral implementation has no constraint on the sampling or geometry of the input data.

INTRODUCTION

Seismic surveys geared to acquiring 3-D data commonly include irregular distribution of common midpoint (CMP) locations. These irregularities in the survey arise from the need for accommodating complex topography and other hazards that exist in the survey area. As a result, Kirchhoff-type algorithms are more popular in processing 3-D seismic data than those faster Fourier approaches, since the integral DMO can handle the irregularly sampled data (Deregowski, 1987). However, triplications in the dip-moveout (DMO) operator, an important phenomenon associated with $v(z)$ media as well as anisotropic media, are difficult to handle using the conventional integral methods. Such limitation exists mainly because a large portion of the energy along the operator can not be accurately predicted by a ray-theoretical construction of the operator in the time-space domain.

Hale and Artley (1993) introduced a 2-D method for approximately handling $v(z)$ model by squeezing the impulse response of the constant-velocity DMO operator. Artley and Hale (1994) proposed an exact 2-D $v(z)$ DMO in the frequency-wavenumber domain, which can solve the problem of triplication by constructing the 2-D parametric DMO operator in the ray parameter domain. Extensions of the parametric DMO operator construction to 3-D or anisotropic media can be found at Artley et al. (1993) and Alkhalifah (1997). Several other methods for precise DMO correction have also been published in the SEG abstract (Meinardus and Schleicher, 1991; Witte, 1991; Perkins and French, 1990). Alkhalifah and deHoop (1996) demonstrated that an integral DMO operator in the $\tau - p$ domain for anisotropic media can solve the problem of triplication, as well as, sampling irregularities.

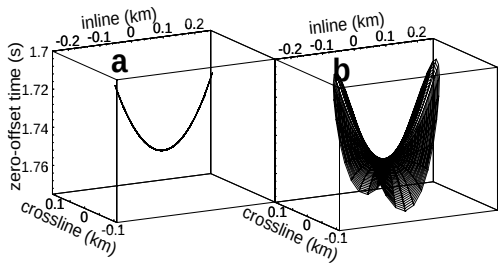

Figure 1: 3-D DMO operator trajectory in the time-space domain. (**a**) Constant velocity. (**b**) $v(z)$ velocity.

It is well-known that the 3-D $v(z)$ DMO operator in the time-space domain is saddle-shaped if we do not take into account of the triplications, as shown in Figure 1. In order to handle the triplications accurately, we propose a 3-D integral DMO approach in the slant-stack domain. This approach starts with constructing the parametric 3-D DMO operator using ray tracing, which is composed of three functions. The three functions are merged into a single function using 3-D slant-stack transform. Each input sample is smeared onto the a panel in the slant-stack domain. Then, an accurate and efficient inverse slant-stack transform is applied to transform the data back to the conventional time-space domain. We plan to extend a 2-D slant-stack transform method developed by Kostov (1990) to 3-D.

We first derive the equations used for constructing the parametric 3-D DMO operator in the ray parameter domain. Then we discuss how to implement the DMO correction in the slant-stack domain. Finally, some numerical results are presented to demonstrate how the proposed operator handles triplications in the slant-stack domain.

CONSTRUCTING PARAMETRIC 3-D DMO OPERATOR

3-D DMO operator in the time-space domain is constructed by solving a system of nonlinear equations. As shown in Figure 2, the source is assumed to be located at the origin. First, all the three rays $\overrightarrow{SR}$,

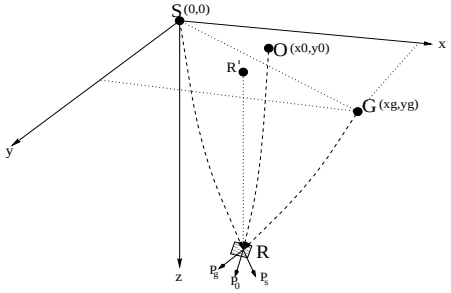

Figure 2: Schematic view of the source **S**, geophone **G**, and reflection point **R** for 3-D $v(z)$ DMO. The dash lines represent the raypaths in the earth.

$\overrightarrow{GR}$, and $\overrightarrow{OR}$ terminate at the same reflection point **R** with the surface location at point $\mathbf{R}'$, i.e.,

$$x(\mathbf{p}_s, t_s) = x(\mathbf{p}_0, t_0) + x_0, \tag{1}$$

$$x(\mathbf{p}_g, t_g) + x_g = x(\mathbf{p}_0, t_0) + x_0, \tag{2}$$

$$y(\mathbf{p}_s, t_s) = y(\mathbf{p}_0, t_0) + y_0, \tag{3}$$

and

$$y(\mathbf{p}_g, t_g) + y_g = y(\mathbf{p}_0, t_0) + y_0, \tag{4}$$

where $\mathbf{p}_i$ stands for the ray parameter vector, t_i represents the one-way traveltime from the surface to the reflection point. Second, all the three rays terminate at $\mathbf{R}$ with the same time-depth, resulting in

$$\tau(\mathbf{p}_s, t_s) = \tau(\mathbf{p}_0, t_0), \tag{5}$$

and

$$\tau(\mathbf{p}_g, t_g) = \tau(\mathbf{p}_0, t_0). \tag{6}$$

Third, all the three rays observe Snell's law at the reflection point **R**. Consequently, the ray parameters are constrained by the following equations,

$$p_0^x \left(\cos\theta(\mathbf{p}_s, t_s) + \cos\theta(\mathbf{p}_g, t_g)\right) = (p_s^x + p_g^x)\cos\theta(\mathbf{p}_0, t_0), \tag{7}$$

and

$$p_0^x\,(\cos\theta(\mathbf{p}_s,t_s)+\cos\theta(\mathbf{p}_g,t_g))=(p_s^x+p_g^x)\cos\theta(\mathbf{p}_0,t_0). \tag{8}$$

Finally, the total traveltime is the sum of the source and the geophone's one-way traveltimes,

$$t_s+t_g=t_{sg}. \tag{9}$$

There are totally nine unknowns, $\mathbf{p}_s=(p_s^x,p_s^y)$, $\mathbf{p}_g=(p_g^x,p_g^y)$, x_0, y_0, t_0, t_s, t_g. By subtracting (2) from (1) and (4) from (3), two independent equations

$$x(\mathbf{p}_s,t_s)=x(\mathbf{p}_g,t_g)+x_g, \tag{10}$$

and

$$y(\mathbf{p}_s,t_s)=y(\mathbf{p}_g,t_g)+y_g. \tag{11}$$

are left. If we substitute equation (9) into (5), we get

$$\tau(\mathbf{p}_s,t_{sg}-t_g)=\tau(\mathbf{p}_0,t_0). \tag{12}$$

As a result, the number of independent equations reduces to six. Newton-Raphson method (Press et al., 1986) is used to solve the system of six nonlinear equations, 10, 11, 6, 12, 7, and 8, generating the parametric 3-D DMO operator in the ray parameter domain, as follows

$$\left\{\begin{array}{lcl} t_0 &=& f_1(t_n,p_x,p_y;h)\\ x_0 &=& f_2(t_n,p_x,p_y;h)\\ y_0 &=& f_3(t_n,p_x,p_y;h)\end{array}\right. \tag{13}$$

where t_n is the NMO-corrected traveltime, (p_x,p_y) is the ray parameter vector, h is the half-offset, t_0 is the zero-offset traveltime, and (x_0,y_0) is the surface location of the zero-offset trace. Figures 3, 4, and 5 show the three parametric functions from a linear $v(z)$ model. The corresponding parameters are half-offset h=1 (km), NMO-corrected traveltime t_n=1 (sec), and the velocity model $v(z)$=1.5 + z (km/s). Ray parameters p_x and p_y vary from 0 to 0.667 (s/km). The flat regions in Figures 3, 4, and 5 are set to be constant to guarantee the stability of Newton-Raphson method. Although t_0 and x_0 are well-defined as a function of the ray parameters, they do not vary monotonously in the p_x direction. In contrast, y_0 varies monotonously in both p_x and p_y direction. Therefore, if the three maps are merged into one in (t_0,x_0,y_0) domain, the triplications are inevitable in the inline direction (at the large p_x).

3-D DMO IN THE SLANT-STACK DOMAIN

Since all the three parametric functions are defined in the ray parameter domain, it is natural to merge them into one single function given by

$$\tau(t_n,p_x,p_y;h)=t_0+x_0p_x+y_0p_y. \tag{14}$$

Figure 6 shows a quarter of the operator trajectory in the 3-D slant-stack domain. This new expression has a simpler behavior in the p_x direction than the conventional time-space expression in the inline direction, since the new expression is simply a linear combination of the three parametric functions. It will be shown in the next section that the operator triplication in the inline direction of the time-space domain becomes an inflection point in the slant-stack domain. Furthermore, even though the parametric DMO operator has triplication information, it is not convenient for application, because the operator is not defined on a regular grid in the (x_0,y_0) domain. Meanwhile, the ray theoretical construction of the operator does not include the true dynamics of the triplication. Direct use of the parametric DMO operator in a conventional Kirchhoff approach will result in severe artifacts. By transforming the operator to the slant-stack domain, our method avoids triplications, and as a result, the dynamic description of the operator becomes trivial. The methodology of applying the operator in the slant-stack domain consists of three main steps:

1. Smear each input sample into the slant-stack domain according to the operator trajectory.
2. Inverse transform the data back to the conventional time-space domain.
3. Kirchhoff summation of the inverse transformed data.

Since the operators are applied independently for each input sample, the proposed DMO algorithm is an integral approach that can handle irregularly sampled data. The key step of this algorithm is an accurate and efficient inverse slant-stack transform. We plan to extend a 2-D slant stack transform method by Kostov (1990) to 3-D. The efficiency of his method results from the observation that the matrix of normal equations has a Toeplitz structure, even for data that are irregularly sampled or non-uniformly weighted in offset, while the accuracy originates from its finite-aperture feature which can reduce the artifact caused by infinite aperture.

NUMERICAL RESULTS

Results from two different $v(z)$ models are presented in this section. The first one is a linear $v(z)$ model, $v(z)=1.5+z$ (km/s); while the second example has a high velocity layer embedded in a general $v(z)$ model, as shown in Figure 7. Figure 8 shows the inline component of the 3-D $v(z)$ DMO operator from the linear $v(z)$ model. Two triplications in the time-space domain have been transformed into two inflection points in the slant-stack domain. A similar phenomenon occurs in anisotropic media between the phase and group velocities (Alkhalifah and deHoop, 1996). Figure 9 shows the crossline component from the 3-D DMO operator of the linear $v(z)$ model. Since the operator is well-known to be saddle-shaped, the crossline component is concaved downward. Consistent with y_0's monotonous trajectory in the ray parameter domain (Figure 5), the crossline component has no triplications and its counterpart is also free of inflection points in the slant-stack domain. Figure 10 shows the inline component of the 3-D DMO operator for the second $v(z)$ model. A little more complexity of the velocity model gives rise to many more triplications in the time-space domain. It is very difficult to use such an operator in the conventional integral DMO, making it necessary to build the operator in the slant-stack domain. As shown in the right plot of Figure 10, all the triplications are transformed to inflection points without exception.

CONCLUSIONS

We developed a new 3-D integral DMO method in the slant-stack domain. Our tests show that the new expression has some significant advantages over the conventional time-space expression. First, the operator triplications in the inline direction of the time-space domain are transformed to be inflection points in the slant-stack domain. Second, the dynamic description of the operator becomes trivial in the slant-stack domain, which can reduce the artifacts caused by triplications. The inverse slant-stack transform step, though maybe time-consuming, is necessary to handle the inherent triplications associated with DMO operators in $v(z)$ media. In spite of using the slant-stack domain, the new approach has not compromised the main features of the conventional integral DMO. Therefore, it is capable of handling irregularly sampled data.

REFERENCES

Alkhalifah, T., and deHoop, M. V., 1996, Integral DMO in anisotropic media: 66th Annual Internat. Mtg., Soc. Expl. Geophys., Expanded Abstracts, 491–494.

Alkhalifah, T., 1997, Kinematics of 3-D DMO operators in transversely isotropic media: Geophysics, **62**, 1214–1219.

Artley, C., and Hale, D., 1994, Dip-moveout processing for depth-variable velocity: Geophysics, **59**, 610–622.

Artley, C., Blondel, P., Popovici, A. M., and Schwab, M., 1993, Equations for three dimensional dip moveout in depth-variable velocity media: SEP–**77**, 43–48.

Deregowski, S. M., 1987, Integral implementation of dip moveout: Geophysical Transactions, **33**, 11–22.

Hale, D., and Artley, C., 1993, Squeezing dip moveout for depth-variable velocity: Geophysics, **58**, 257–264.

Kostov, C., 1990, Toeplitz structure in slant-stack inversion: 60th Annual Internat. Mtg., Soc. Expl. Geophys., Expanded Abstracts, 1618–1621.

Meinardus, H. A., and Schleicher, K., 1991, 3-d time-variant dip-moveout by the fk method: 61st Annual Internat. Mtg., Soc. Expl. Geophys., Expanded Abstracts, 1208–1210.

Perkins, W. T., and French, W. S., 1990, 3-d migration to zero offset for a constant velocity gradient: 60th Annual Internat. Mtg., Soc. Expl. Geophys., Expanded Abstracts, 1354–1357.

Press, W. H., Teukolsky, B. P. F. S. A., and Vetterling, W. T., 1986, Numerical recipes: Cambridge University Press.

Witte, D., 1991, Dip moveout in vertically varying media: 61st Annual Internat. Mtg., Soc. Expl. Geophys., Expanded Abstracts, 1181–1183.

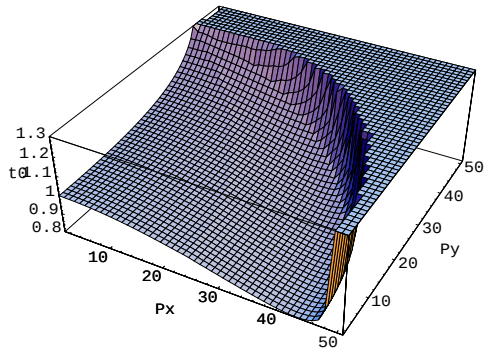

Figure 3: Parametric 3-D DMO operator, t_0=$f_1(t_n, p_x, p_y; h)$. Although t_0 is well-defined in (p_x,p_y) domain, it does not vary monotonously in the p_x direction. The flat range is set to be constant to guarantee the stability of Newton-Raphson method.

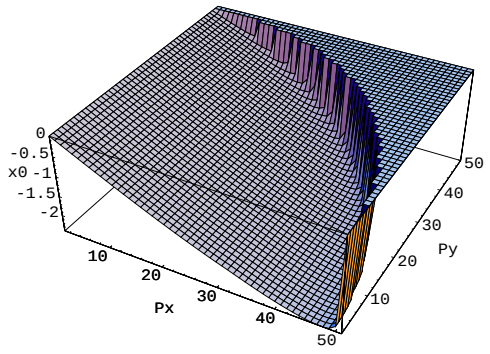

Figure 4: Parametric 3-D DMO operator, x_0=$f_2(t_n, p_x, p_y; h)$, using the same parameter as Figure 3.

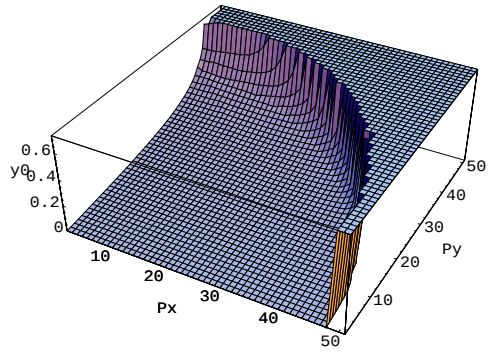

Figure 5: Parametric 3-D DMO operator, y_0=$f_3(t_n, p_x, p_y; h)$, using the same parameter as Figure 3.

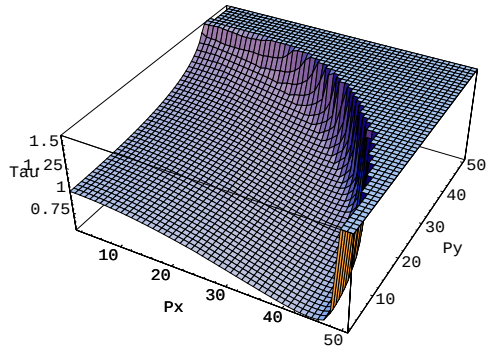

Figure 6: 3-D DMO operator $\tau(t_n, p_x, p_y; h)$ in the slant-stack domain using the same parameter as Figure 3.

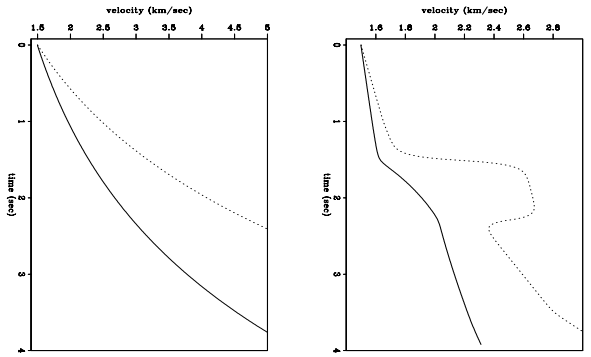

Figure 7: **Left**: Linear velocity model. **Right**: $v(z)$ model with a high velocity disturbance. The dash line stands for the interval velocity and the solid line for the RMS velocity.

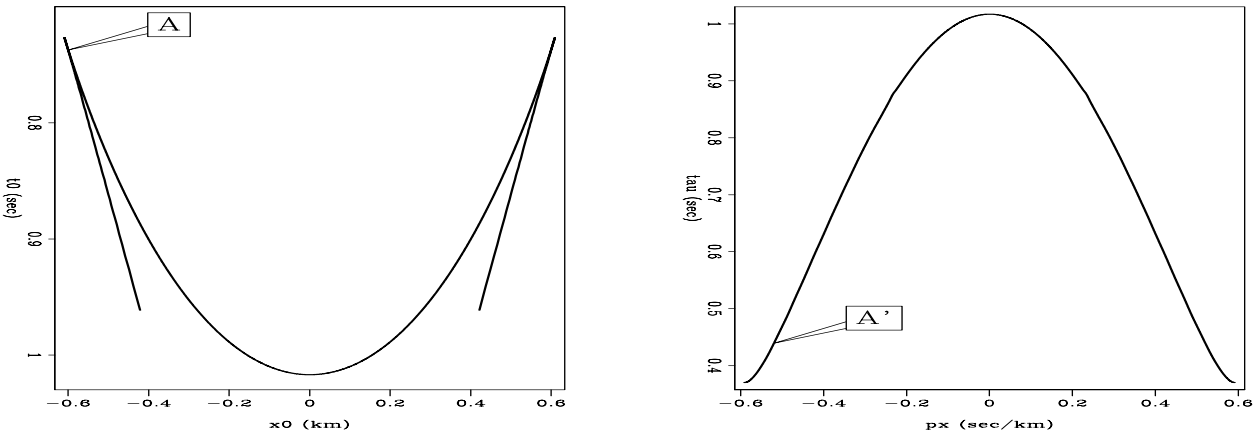

Figure 8: 3-D DMO operator trajectory in the inline direction. **Left**: (t_0, x_0) domain (y_0=0). **Right**: (τ, p_x) domain (p_y=0). A represents the triplication in the time-space domain. $A^{'}$ points to the inflection point in the slant-stack domain. This figure corresponds to the linear $v(z)$ model.

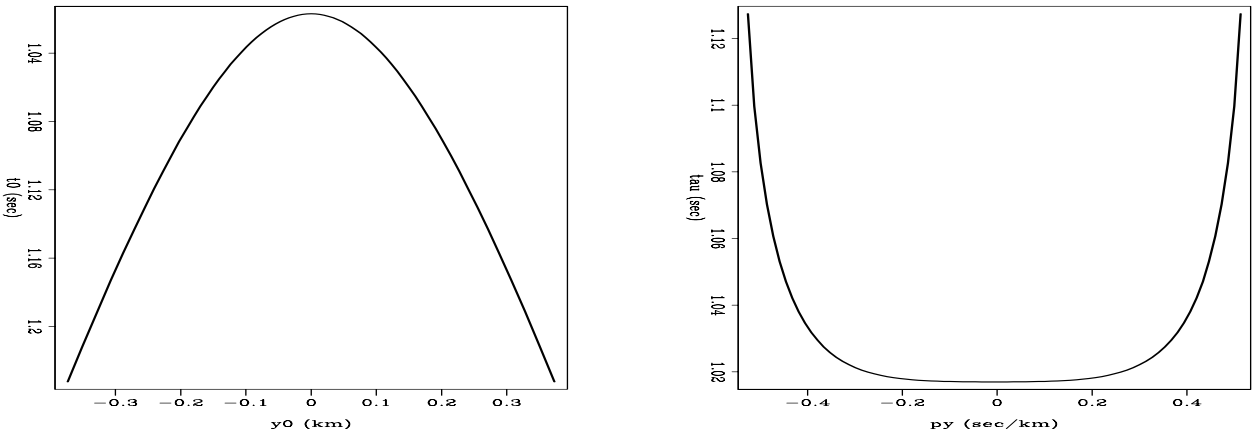

Figure 9: 3-D DMO operator trajectory in the crossline direction. **Left**: (t_0, y_0) domain (x_0=0). **Right**: (τ, p_x) domain (p_y=0). This figure corresponds to the linear $v(z)$ model.

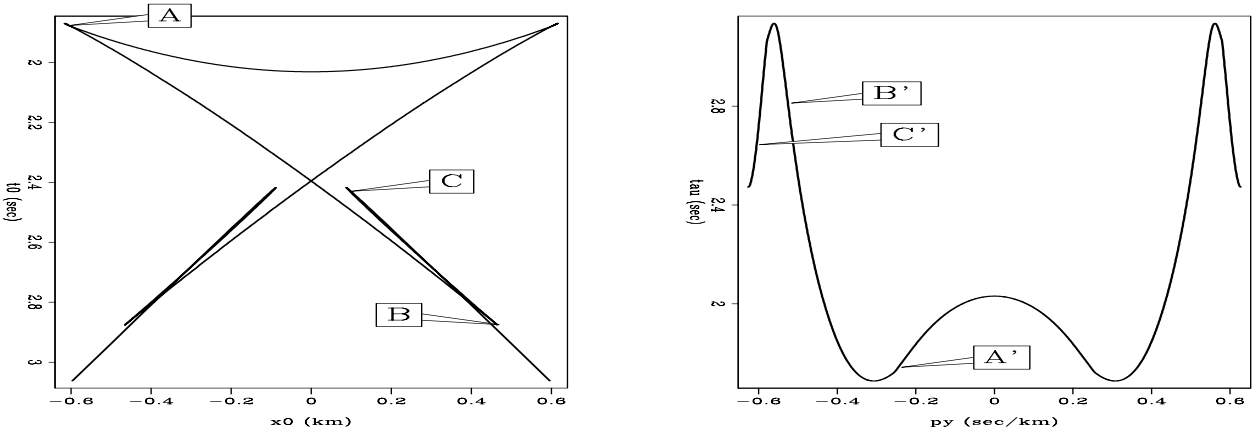

Figure 10: 3-D DMO operator trajectory in the inline direction. **Left**: (t_0, x_0) domain (y_0=0). **Right**: (τ, p_x) domain (p_y=0). A, B, and C refer to the tripilcations in the time-space domain. $A^{'}$, $B^{'}$, and $C^{'}$ point to the inflection points in the slant-stack domain. This figure is from the second example.